Expanded View Figures

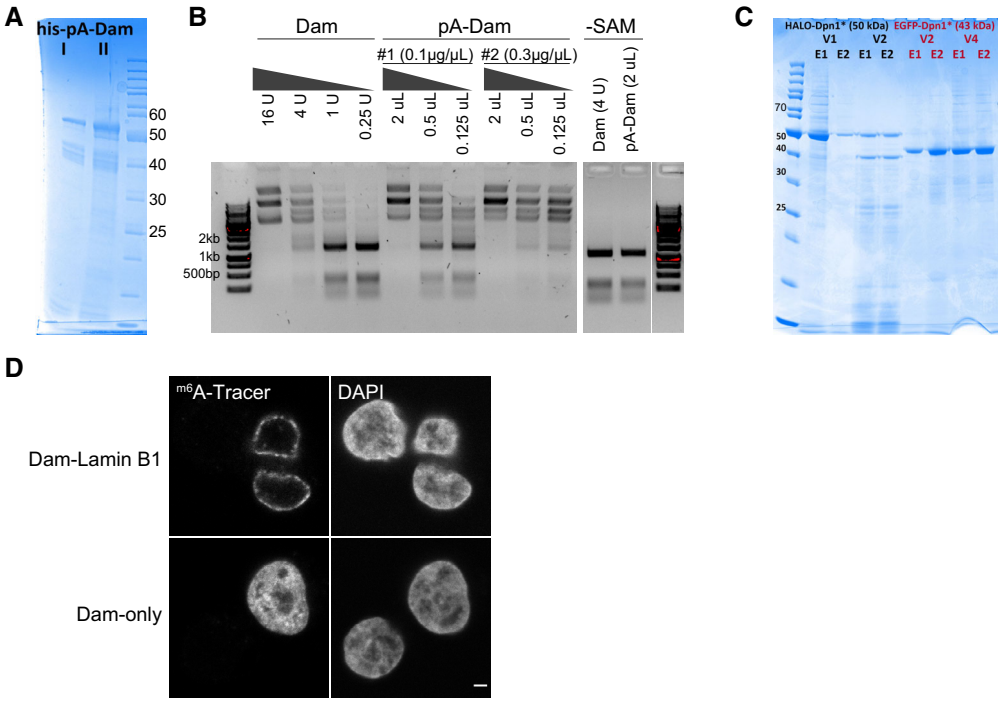

Figure EV1. Production and validation of the pA-DamID proteins.

A SDS–PAGE gel of two batches of bacterial purified pA-Dam protein (expected molecular weight: 52 kDa) with concentrations of ~0.1 and ~0.3 µg/µl, respectively.

B Agarose gel analysis of Mbo I protection assay. Unmethylated plasmid is ^{m6}A methylated by a range of Dam and pA-Dam concentrations. The DNA is subsequently digested by Mbo I, which can cut GATC but not G^{m6}ATC sequences. The pA-Dam batches have Dam activities estimated to be ~8 and ~32 units (see Materials and Methods for definition) per ~0.1 µg and ~0.3 µg pA-Dam protein, respectively. No Mbo I protection is observed without the methyl donor SAM.

C SDS–PAGE gel of ^{m6}A-Tracer protein purified from insect cells, with the truncated DpnI fused to EGFP and HALO tags. Two elutions (labeled E1/E2) obtained with two independent baculovirus pools (labeled V1/V2 and V2/V4) produced protein of the expected size (50 and 43 kDa for EGFP and HALO-tagged protein, respectively) and were pooled.

D Confocal sections of ^{m6}A-Tracer signal in HAP-1 cells transduced with lentivirus expressing Dam-Lamin B1 (*top panel*) and Dam-only (*bottom panel*). Negative cells are presumably non-transduced cells. The scale bar corresponds to 2 µm.

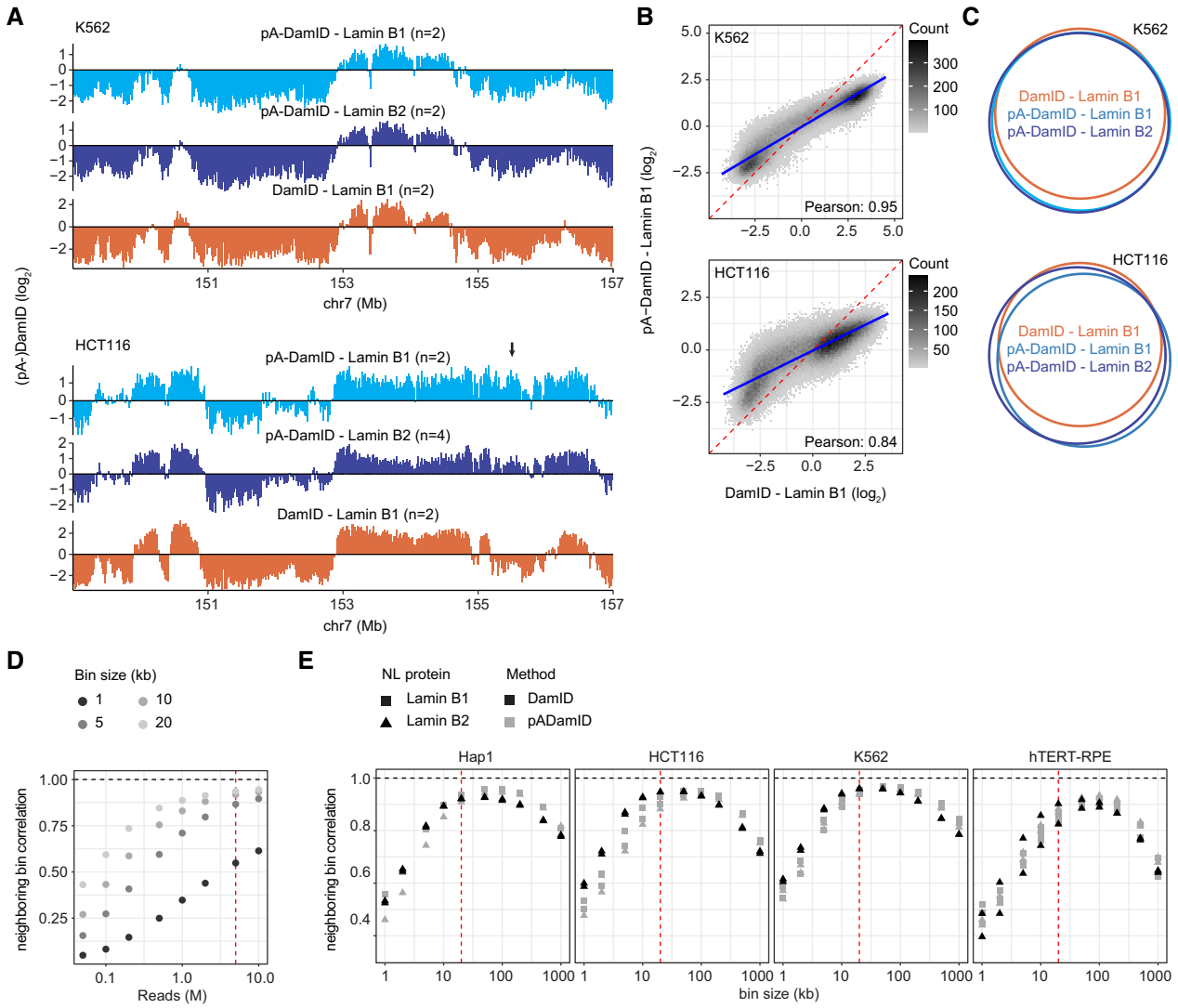

Figure EV2. Comparison of NL interactions determined by pA-DamID and DamID for K562 and hTERT-RPE cells.

A–C Plots similar to Fig 3A–C, but for K562 and HCT116 cells. Data are averages of *n* biological replicates (see panel A). Arrow indicates a region with dissimilar pA-DamID and DamID scores (panel A). The blue line represents a linear model, and the red dashed line represents the diagonal (panel B).

D Pearson correlation coefficients between neighboring bins on chromosome 1 for different bin sizes, calculated for increasing numbers of sequence reads that end in GATC. The red line highlights 5 million Lamin B2 and 5 million Dam counts, which is used in panel (E). Data are from Replicate 1 of Lamin B2 pA-DamID in K562 cells.

E Correlation between neighboring bins on chromosome 1 for pA-DamID data downsampled to 5 million Lamin B2 and 5 million Dam sequence reads, calculated for various bin sizes. All pA-DamID and DamID experiments for Lamin B1 and Lamin B2 are included that had sufficient read counts. The red line highlights the 20 kb bin size, which is used throughout this report.

Figure EV3. Analysis of NL interactions at various times after mitosis.

A Synchronized cells were fixed on poly-L-lysine-coated cover slips and stained with DAPI. Percentage of mitotic cells was estimated by visual scoring of metaphase and anaphase appearance in confocal microscopy images. 207 and 82 cells were assessed in the two replicates (r1, r2), respectively.

B Ratio of gel intensities from amplified ^{m6}A fragments between Lamin B2 pA-DamID and Dam control, normalized for input DNA. For the second replicate, input DNA was very low for the time points and could not be determined accurately. These samples thus show a large variation in amplification ratio compared with the first replicate. The 0 h time point consistently shows low amplification ratios, similar to unsynchronized samples without a primary antibody. This indicates that genome–NL interactions at this time point are very weak.

C Data distribution before and after scaling to z-scores. The distributions are not affected by this transformation. Every line represents a single replicate.

D Density plots of propidium iodide (PI) signals of hTERT-RPE cells following mitotic shake-off and replating *(left)*. Example light microscopy of hTERT-RPE cells following replating *(right)*. The scale bar corresponds to 100 μm.

E Overview of the classification of dynamic LADs. LADs were defined for every time point by selecting LADs that are called in both replicates using hidden Markov modeling, after which a union across time points was used as consensus LAD definition. For every LAD, per-bin z-score differences are calculated between 1 h and 21 h, and a line is drawn between the 25th and 75th percentiles of these values. This shows that numerous LADs change as complete units between 1 h and 21 h. The right panel shows the same figure, but is colored by LAD classification into stable and dynamic using limma-voom differential analysis (Materials and Methods).

F Read counts for Dam and Lamin B2 (normalized for overall sequencing read depth) were calculated for stable and dynamic LADs. Plotted are $\log_2$-ratios relative to the 1 h time point. This shows that Dam reads do not change between time points. Average two of biological replicates. Boxplots: horizontal lines represent 25th, 50th, and 75th percentiles; whiskers extend to the smallest values no further than 1.5 times distance between 25th and 75th percentiles.

G Similar figure as Fig 4I, showing distance to centromeres instead.

H LAD size is not correlated with distance to telomeres (Pearson correlation coefficient: 0.01). The blue dashed line represents a linear model.

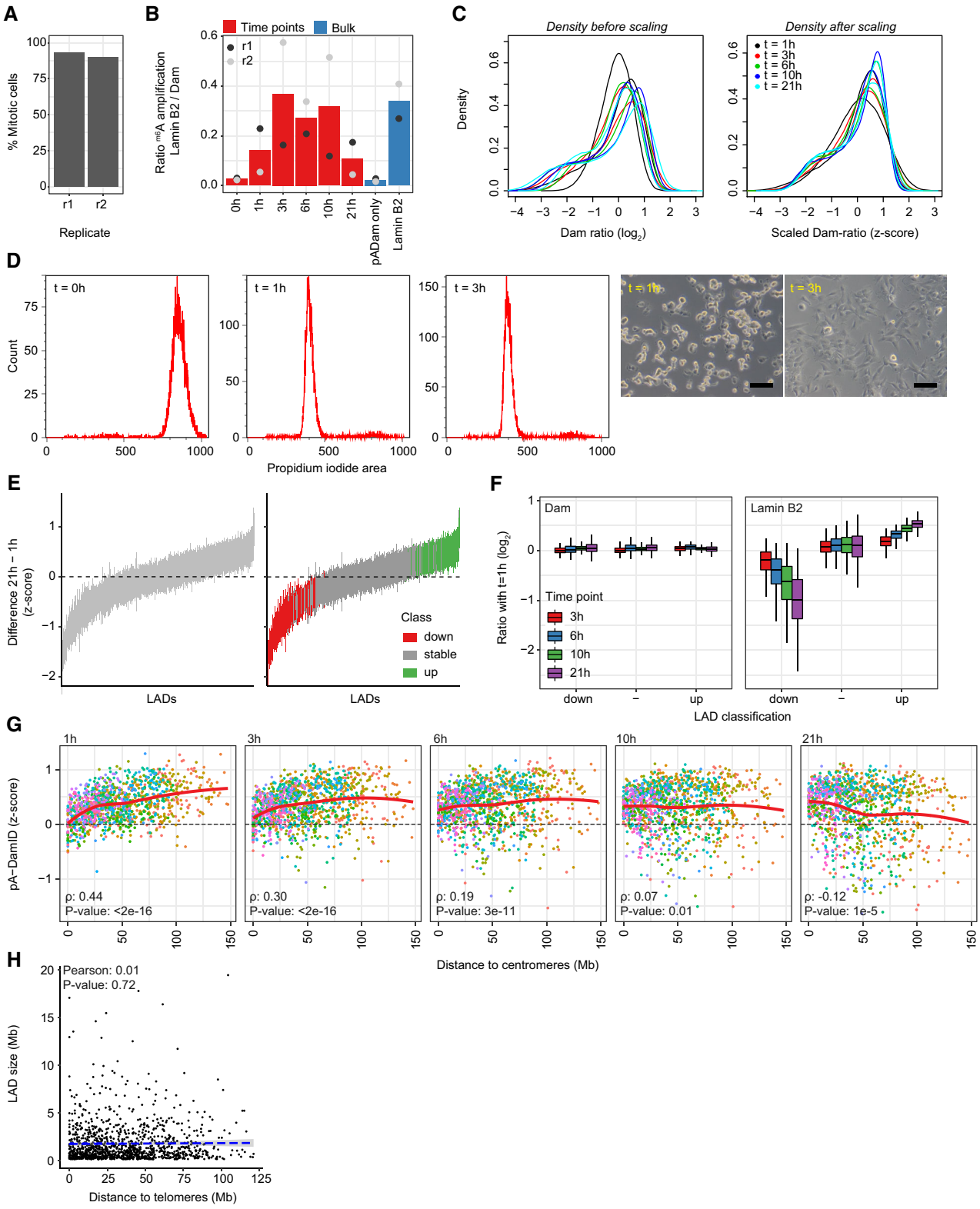
A
% Mitotic cells
Replicate
r1
r2
B
Time points
Bulk
r1
r2
Ratio m6A amplification Lamin B2 / Dam
0h
1h
3h
6h
10h
21h
pADam only
Lamin B2
C
Density before scaling
Density after scaling
Density
Dam ratio (log2)
Scaled Dam-ratio (z-score)
t = 1h
t = 3h
t = 6h
t = 10h
t = 21h
D
t = 0h
t = 1h
t = 3h
Count
Propidium iodide area
E
Difference 21h – 1h (z-score)
LADs
Class
down
stable
up
F
Dam
Lamin B2
Ratio with t=1h (log2)
Time point
3h
6h
10h
21h
down
–
up
LAD classification
G
1h
3h
6h
10h
21h
pA–DamID (z-score)
ρ: 0.44
P-value: <2e-16
ρ: 0.30
P-value: <2e-16
ρ: 0.19
P-value: 3e-11
ρ: 0.07
P-value: 0.01
ρ: -0.12
P-value: 1e-5
Distance to centromeres (Mb)
H
Pearson: 0.01
P-value: 0.72
LAD size (Mb)
Distance to telomeres (Mb)

Figure EV3.

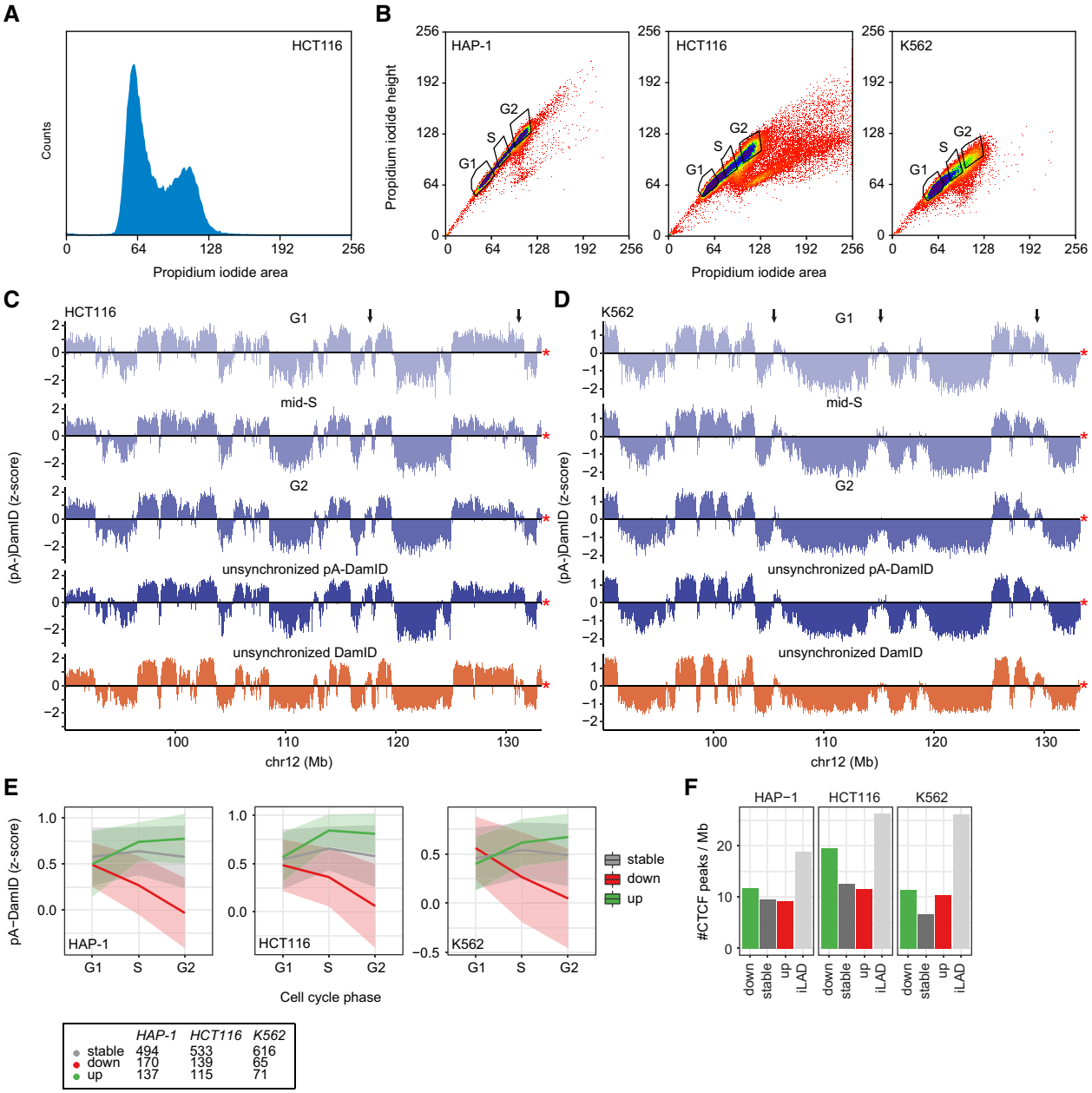

	HAP-1	HCT116	K562
stable	494	533	616
down	170	139	65
up	137	115	71

Figure EV4. LAD dynamics in flow sorted HCT116 and K562 cells.

A Density plot of propidium iodide (PI) signals of HCT116 cells after application of the pA-DamID protocol and PI staining.

B Sorting strategy of pA-DamID processed cells stained PI. Single cells were selected based on PI height and area and sorted into three pools: G1, mid-S, and G2. G1 and G2 gates were set around the two PI peaks (see also A). The mid-S gate was set to covering intermediate PI signals, clearly distinct from the G1 and G2 peaks. For every condition, 2 or 3 wells were filled with 1,000 cells and processed to generate one sequencing library.

C, D Same locus as Fig 5A for HCT116 (C) (n = 2) and K562 cells (D) (n = 2). The arrows highlight dynamic regions. The red asterisk indicates the end of the chromosome.

E Similar plot as Fig 4C, with cell cycle stages on the x-axis. The numbers of stable and dynamic LADs are shown for the three cell types.

F CTCF ChIP-seq peak density per Mb for stable and dynamic LADs. iLADs are defined as genomic regions not overlapping with stable or dynamic LADs. CTCF data are from (Consortium EP, 2012; Haarhuis *et al*, 2017). A permutation test with 1,000 permutations (R-package *regioneR* (Gel *et al*, 2016)) was used to test for a significant enrichment of CTCF peaks in decreasing LADs, resulting in P-values of 1e-3, 1e-3, and 1e-3 for HCT116, HAP-1, and K562, respectively.

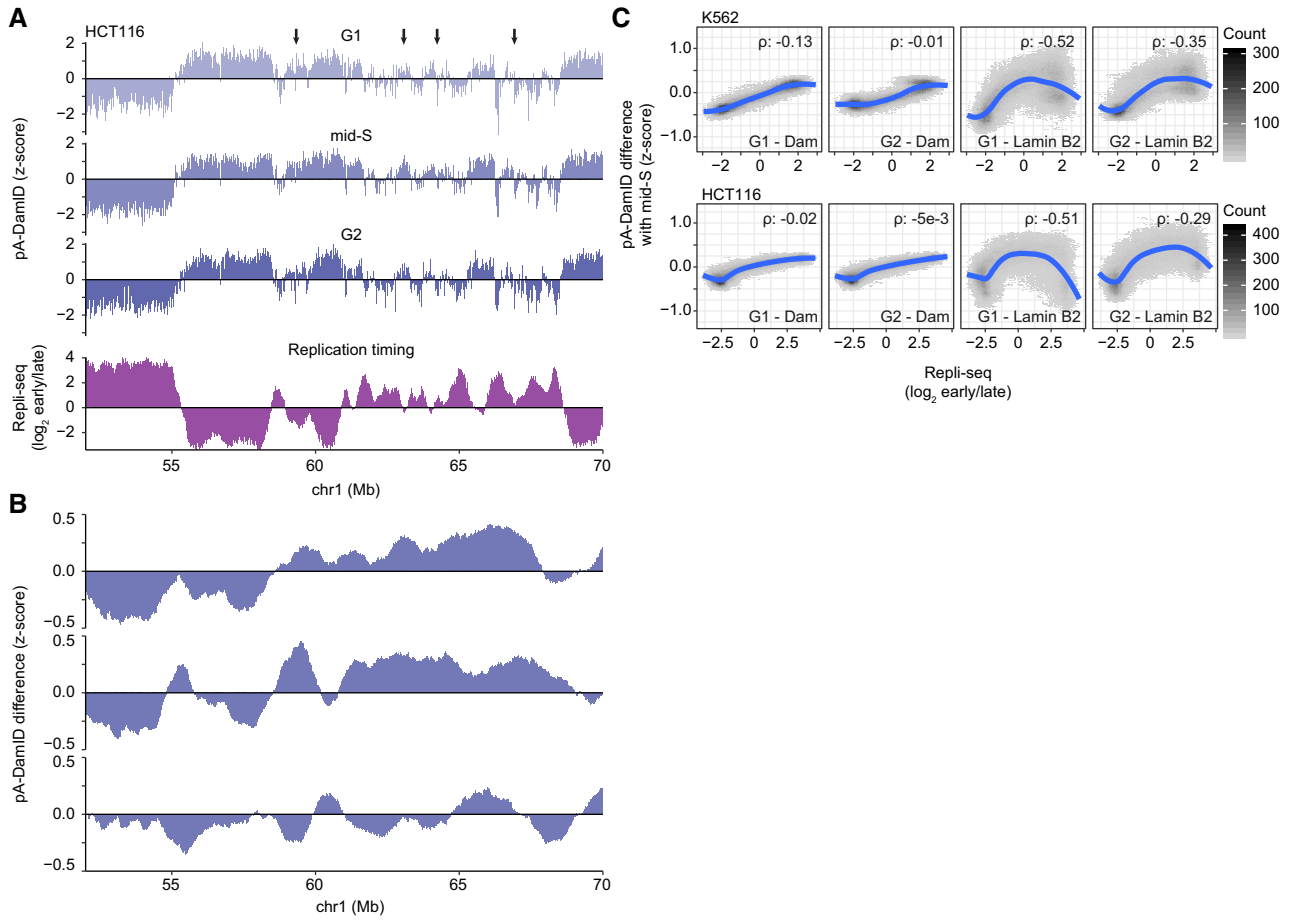

Figure EV5. Transiently increased Lamin B2 interactions during mid-S are not due to increased Dam reads.

A, B Similar figures as Fig 6A and B for a locus in HCT116 cells. Arrows highlight regions with increased mid-S signal compared with G1 and G2. Average of two biological replicates.

C Similar plot as Fig 6C, showing the difference in read-normalized counts for Dam and Lamin B2 samples. This plot shows a gradual increase in S-phase enrichment for Dam reads, reflecting DNA duplication of early replicating DNA. In contrast, Lamin B2 reads show an increase in S-phase enrichment for Repli-seq scores around 0, reflecting mid-S chromatin. The Lamin B2 Spearman correlation coefficients are significantly higher than for Dam ($P < 2e\text{-}16$ for both G1 and G2, William's *t*-test using R-package *cocor*; Diedenhofen & Musch, 2015). Repli-seq data are from the 4D Nucleome data repository (https://data.4dnucleome.org) (Dekker *et al*, 2017).